Bandwidth Behavior of Omnidirectional Dual-Reflector Antennas Synthesized for Uniform Coverage

José R. Bergmann* and Fernando J. S. Moreira
**CETUC, PUC-Rio - Av. Marquês de São Vicente 225 - Rio de Janeiro, RJ - CEP 22453-900, Brazil*
Dept. Electronics Engineering, UFMG, Belo Horizonte, MG, CEP 31270-901, Brazil

Abstract— **This work presents a study on the electromagnetic behavior of omnidirectional dual-reflector antennas synthesized to provide uniform coverage. Special attention is paid to the antenna radiation pattern across a 10% bandwidth, in order to establish limits for the applicability of omnidirectional dual-reflector antennas in broadband communication services. Several case studies involving classical and shaped configurations are investigated. The results are validated by method-of-moments analysis.**

Index Terms— Reflector antennas, omnidirectional dual-reflector antennas, reflector antenna shaping.

I. INTRODUCTION

Broadband wireless access offers flexible connectivity to communication services demanding large transmission rates. Several systems, like WiMax, are based on the cellular concept where a specific region (cell) is covered by a radio base station. This coverage may be provided by several antennas, in which case each cell sector is covered by a single antenna, or by a single omnidirectional antenna. In microwaves and millimeter-waves, reflector antennas are usually employed. Many studies have been conducted in order to establish efficient reflector configurations to provide omnidirectional coverage [1-8]. Such omnidirectional reflectors are composed by circularly symmetric surfaces (or bodies of revolution—BOR's) that may be generated by conic sections or shaped generatrices. Together with the feed radiation characteristics, the reflector system controls the omnidirectional radiation pattern of the antenna in the elevation plane.

Several works have already dealt with shaping of omnidirectional reflector arrangements in the past. For instance, omnidirectional single reflectors were investigated in [5]. Although simpler, single reflectors have larger diameters when compared with dual-reflector configurations. Dual-reflector arrangements with virtual subreflector caustic were investigated in [1-4]. In principle, such antennas may have large feed return losses [6]. In order to reduce the feed return loss, while providing more design options, generalized studies were conducted in [6-8] to establish all possible dual-reflector configurations providing omnidirectinal coverage. Among the possible configurations, those based on the axis-displaced Cassegrain (ADC) and axis-displaced ellipse (ADE) may provide compact dual-reflector arrangements and, for this reason, are considered in the present work.

Brazilian Microwave and Optoelectronics Society-SBMO received 25 Nov., 2008; revised 3 Feb., 2009; accepted 24 March, 2009
Brazilian Society of Electromagnetism-SBMag *ISSN 1516-7399*

The present work investigates the behavior of the radiation pattern of omnidirectiona dual-reflector antennas across a 10% bandwidth. Special attention is dedicated to omnidirectional ADC and ADE antennas. Both classical and shaped reflector arrangements are considered. The objective of such investigation is to determine the effects of the main-reflector shaping on the operation bandwidth of these antennas.

II. CLASSICAL OMNIDIRECTIONAL ADC AND ADE DUAL-REFLECTOR ANTENNAS

Initially, the behavior of classical ADC and ADE omnidirectional antennas is investigated, with classical meaning that the sub- and main-reflector BOR surfaces are generated by conic sections. For the ADC configuration (Fig. 1a) the subreflector is generated by a hyperbola and the main-reflector is generated by a parabola. As a consequence, the subreflector has a virtual ring caustic (represented by *P* in Fig. 1a). On the other hand, the ADE antenna has a subreflector generated by an ellipse and its ring caustic is real (*P* in Fig. 1b). The main consequence of the real ring caustic between the ADE sub- and main-reflectors is the inversion of the feed illumination toward the main-reflector, which may be a convenient choice for the antenna designer.

The antenna geometric parameters and the design procedure of the ADC and ADE classical configurations are extensively discussed in [6-8]. Here we will only notice that the antenna main-beam direction is controlled by the angle γ, which corresponds to the direction of the generating parabola axis (Fig. 1).

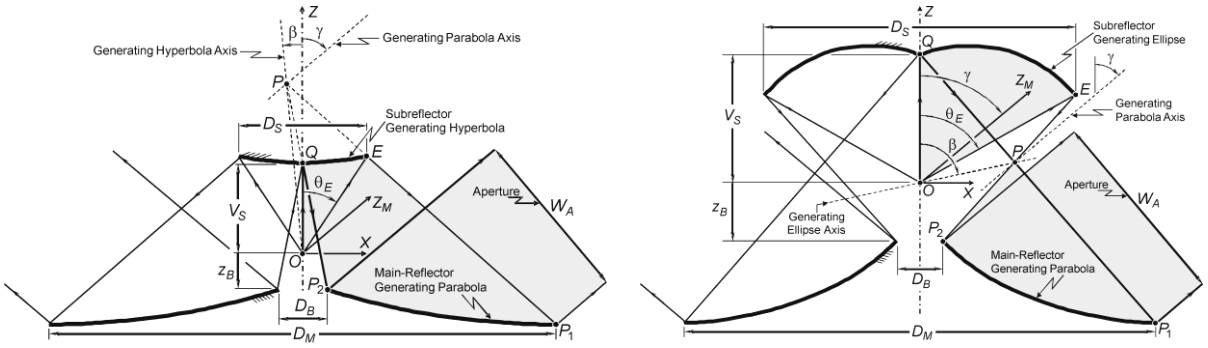

Fig. 1. Classical omnidirectional (a) ADC and (b) ADE dual-reflector antennas.

In order to investigate the behavior of the radiation characteristics across a 10% bandwidth, the omnidirectional ADC and ADE antennas with $\gamma = 102°$ of Reference [8] were analyzed. The classical dual-reflector geometries are illustrated in Fig. 2. The necessary procedure to obtain these dual-reflector arrangements are detailed in [8]. In order to validate the design procedure, which is based on geometrical optics (GO) approximations, and to investigate the behavior of the antenna radiation pattern with the frequency variation, full-wave method-of-moments (MoM) analyses were conducted for the ADC and ADE antennas illustrated in Fig. 2 at the relative frequencies 0.95 f_o, f_o,

Brazilian Microwave and Optoelectronics Society-SBMO received 25 Nov., 2008; revised 3 Feb., 2009; accepted 24 March, 2009
Brazilian Society of Electromagnetism-SBMag *ISSN 1516-7399*

and 1.05 f_o, corresponding to a 10% bandwidth. The corresponding MoM radiation patterns are illustrated in Fig. 3. As expected, the main beam is directed toward $\theta \approx \gamma = 102°$. From the ADC radiation patterns depicted in Fig. 3a one observes that the antenna directivity at $\theta = 102°$ is 10.46 dBi, 10.93 dBi, and 10.50 dBi at 0.95 f_o, f_o, and 1.05 f_o, respectively. From Fig. 3b, the ADE directivities at 0.95 f_o, f_o, and 1.05 f_o are 9.46 dBi, 9.64 dBi, and 8.92 dBi, respectively. So, the maximum variation in gain across the 10% bandwidth is about 0.7 dB and is basically due to the variation of the radiation pattern of the TEM coaxial horn with frequency. The results illustrated in Fig. 3 exemplify the bandwidth behavior of the radiation pattern of omnidirectional dual-reflector systems designed from GO principles.

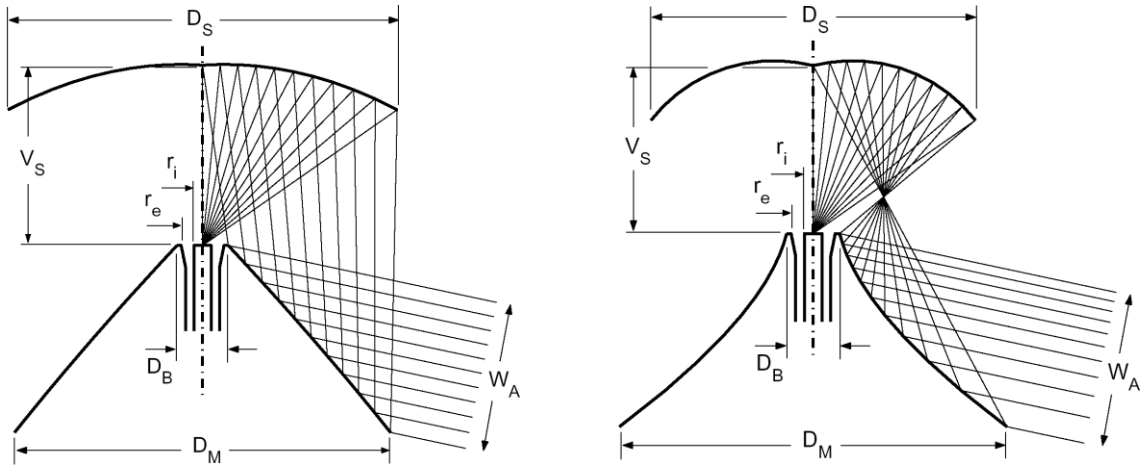

(a) (b)

Fig. 2. Classical omnidirectional (a) ADC and (b) ADE dual-reflector antennas with $\gamma = 102°$, $W_A = 7\lambda_o$, $D_M = 17.56\lambda_o$, $D_B = 2.4\lambda_o$, $z_B = 0$, and $\theta_E = 55°$, fed by a TEM coaxial horn with $r_e = 1\lambda_o$ and $r_i = 0.4\lambda_o$, where λ_o is the wavelength corresponding to the central frequency f_o [8].

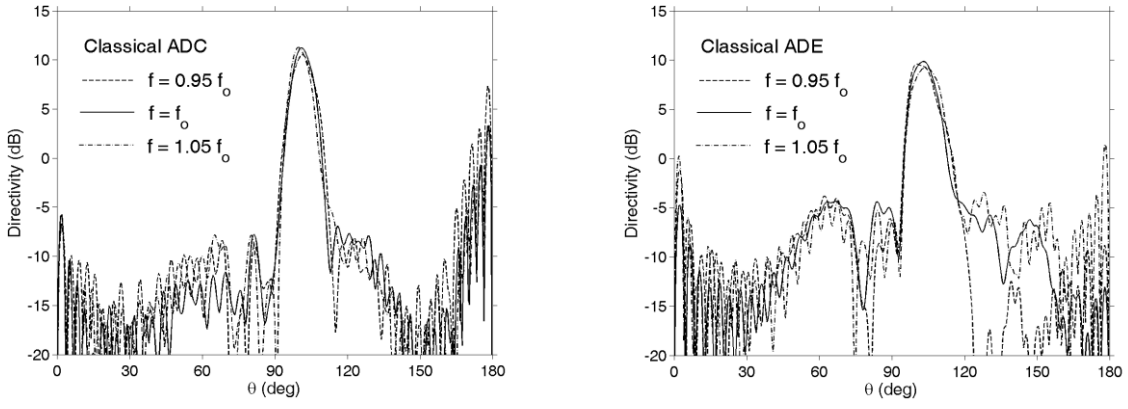

(a) (b)

Fig. 3. Radiation patterns of the classical omnidirectional antennas depicted in (a) Fig. 2a and (b) Fig. 2b at the relative frequencies 0.95 f_o, f_o, and 1.05 f_o (MoM analyses).

Brazilian Microwave and Optoelectronics Society-SBMO *received 25 Nov., 2008; revised 3 Feb., 2009; accepted 24 March, 2009*
Brazilian Society of Electromagnetism-SBMag *ISSN 1516-7399*

III. OMNIDIRECTIONAL ADC AND ADE DUAL-REFLECTOR ANTENNAS WITH SHAPED MAIN-REFLECTOR

Many works have dealt with the shaping of omnidirectional reflector antennas [1,3,5]. We have adopted a procedure where only the main-reflector is shaped to yield a uniform coverage in the elevation plane. The classical subreflector is obtained from the formulation presented in [6-8]. The main-reflector shaping is based on the single-reflector procedure described in [9], suited to handle the present circularly-symmetric main-reflector surfaces.

Following the complex notation of [9] and with the help of Figs. 4 and 5, the main-reflector generatrix is described by:

$$\bar{r}_M(\theta_S) = \left[\rho_P + 2\eta_S e^{L(\eta_S)}\right]\hat{\rho} + \left[z_P + \left(\eta_S^2 - 1\right)e^{L(\eta_S)}\right]\hat{z}, \tag{1}$$

where ρ_P and z_P are the coordinates of the subreflector conic focus P and

$$\eta_S = \cot\left(\frac{\theta_S}{2}\right) \tag{2}$$

represents the direction θ_S of the ray departing from the subreflector toward the main-reflector (see Figs. 4 and 5). For the main-reflector shaping, it is necessary to establish a relation between the feed ray direction θ_F and θ_S, accomplished with the help of the polar equation of the subreflector generating conic [9]:

$$\eta_S = \frac{\varepsilon\cos\beta + 1 - \eta_F\varepsilon\sin\beta}{\varepsilon\sin\beta + \eta_F(\varepsilon\cos\beta - 1)}, \tag{3}$$

where

$$\eta_F = \cot\left(\frac{\theta_F}{2}\right), \tag{4}$$

and ε and β are the eccentricity and the axis tilt angle (see Fig. 2) of the subreflector conic section, respectively. It is interesting to note that (3) is valid for both ADC and ADE antennas. The function $L(\eta_S)$ that describes the main-reflector from (1) is obtained by forcing the main-reflector to obey Snell's law [9]:

$$\frac{\partial L(\eta_S)}{\partial \eta_S} = \frac{2}{\eta - \eta_S}, \tag{5}$$

where

$$\eta = \cot\left(\frac{\theta}{2}\right). \tag{6}$$

The factor 2 in (5) is due to the circular symmetry of the main reflector.

Brazilian Microwave and Optoelectronics Society-SBMO received 25 Nov., 2008; revised 3 Feb., 2009; accepted 24 March, 2009
Brazilian Society of Electromagnetism-SBMag *ISSN 1516-7399*

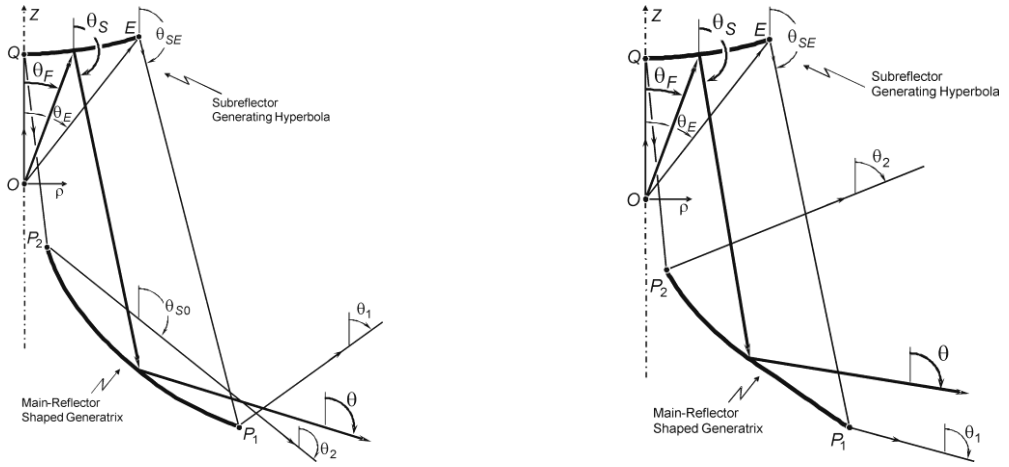

Fig. 4. Generatrices of ADC configurations. Subreflector generated by a hyperbola and main-reflector generated by a shaped generatrix with (a) real caustic and (b) virtual caustic.

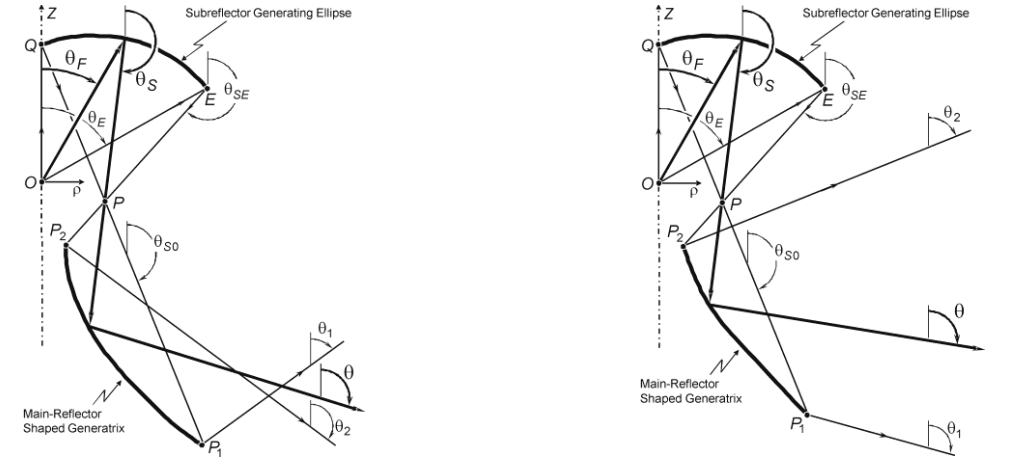

Fig. 5. Generatrices of ADE configurations. Subreflector generated by an ellipse and main-reflector generated by a shaped generatrix with (a) real caustic and (b) virtual caustic.

The main-reflector synthesis is attained by the numerical solution of (5). For this, it is necessary to establish the relation between the ray directions θ (represented by η) and θ_F. This is accomplished by applying the conservation of energy to the bundle of rays that leaves the feed and propagates toward the antenna far-field region after reflecting at both reflectors. According to GO principles, the conservation of energy can be stated as [9]:

$$\int_0^{\theta_F} G_F\left(\theta_F'\right)\sin\theta_F'\, d\theta_F' = N\int_{\theta_1}^{\theta} G_A\left(\theta'\right)\sin\theta'\, d\theta', \tag{7}$$

where $G_F(\theta_F)$ is the feed radiation pattern and $G_A(\theta)$ is the desired radiation pattern of the dual-reflector antenna. In (7), N is simply a normalization factor that equals the total antenna far-field power to the feed power.

Brazilian Microwave and Optoelectronics Society-SBMO received 25 Nov., 2008; revised 3 Feb., 2009; accepted 24 March, 2009
Brazilian Society of Electromagnetism-SBMag *ISSN 1516-7399*

In this work the shaping procedure previously detailed was applied to the antenna main-reflector in order to obtain an omnidirectional radiation pattern with uniform coverage in the elevation plane, which was accomplished by setting the main-reflector to radiate a squared cosecant pattern of the form [10]:

$$G_A(\theta) = A\csc^2(\theta - \pi/2), \qquad \theta \in [\theta_1, \theta_2], \tag{8}$$

where A is a normalization factor and θ_1 and θ_2 are the angular limits of the bundle of rays reflected toward the far-field region (see Figs. 4 and 5). The far-field limiting directions θ_1 and θ_2 also control the behavior of the main-reflector caustic. If $\theta_1 < \theta_2$ then the main-reflector caustic is real, as illustrated in Figs. 4a and 5a for the ADC and ADE configurations, respectively. Otherwise, the caustic is virtual (Figs. 4b and 5b). The squared cosecant pattern of (8) may be desired, for instance, in scenarios where the dual-reflector antenna operates as a base-station antenna.

The adopted feed is a TEM coaxial horn with the same characteristics of that employed in [5]. Its radiation pattern was modeled as:

$$G_F(\theta_F) = B\left[\frac{J_0(kr_i\sin\theta_F) - J_0(kr_e\sin\theta_F)}{\sin\theta_F}\right]^2, \quad \theta_F \le \pi/2, \tag{9}$$

where B is a normalization factor and $k = 2\pi/\lambda$. Equation (9) represents the radiation from a coaxial aperture mounted on a perfect electric conductor plane, with internal and external radii r_i and r_e, respectively. In the results presented below, $r_i = 0.45\lambda_0$ and $r_e = 0.9\lambda_0$, where λ_0 is wavelength of central frequency [5]. As the dimensions of the coaxial-horn aperture are small compared to the wavelength, one should expect the feed phase center to be located close to the horn's aperture plane.

Two case studies are presented here. One comprises an ADC configuration, whose shaped main-reflector has a virtual caustic, as depicted in Fig. 6a. Its subreflector is that of the classical ADC configuration previously analyzed (shown in Fig. 2a). The other configuration is an ADE with a shaped main-reflector with a real caustic (see Fig. 6b), whose subreflector is that of the classical ADE antenna depicted in Fig. 2b. Some relevant dimensions of these antennas are listed in Table I.

Table I – Dimensions of the shaped omnidirectional ADC and ADE antennas of Figs. 6a and 6b, respectively. λ_o is the wavelength corresponding to the central frequency f_o.

Dimension	Shaped ADC	Shaped ADE
D_M	14.48 λ_o	17.56 λ_o
D_S	14.71 λ_o	18.19 λ_o
D_B	2.40 λ_o	2.40 λ_o
V_M	7.45 λ_o	8.53 λ_o
V_S	7.64 λ_o	8.46 λ_o
θ_E	55°	55°

Brazilian Microwave and Optoelectronics Society-SBMO *received 25 Nov., 2008; revised 3 Feb., 2009; accepted 24 March, 2009*
Brazilian Society of Electromagnetism-SBMag *ISSN 1516-7399*

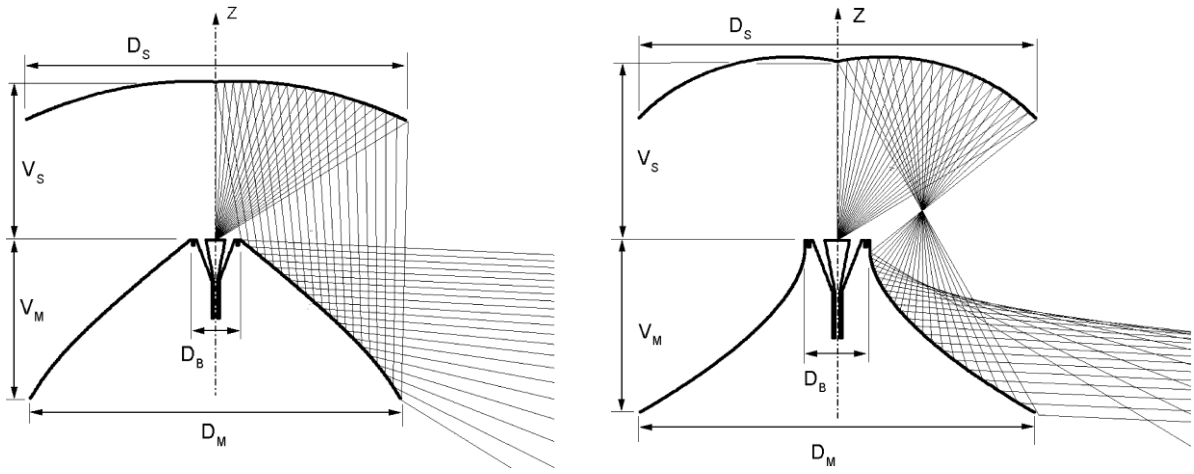

(a) (b)

Fig. 6. Shaped omnidirectional (a) ADC and (b) ADE antennas. The main-reflectors have (a) virtual and (b) real caustics.

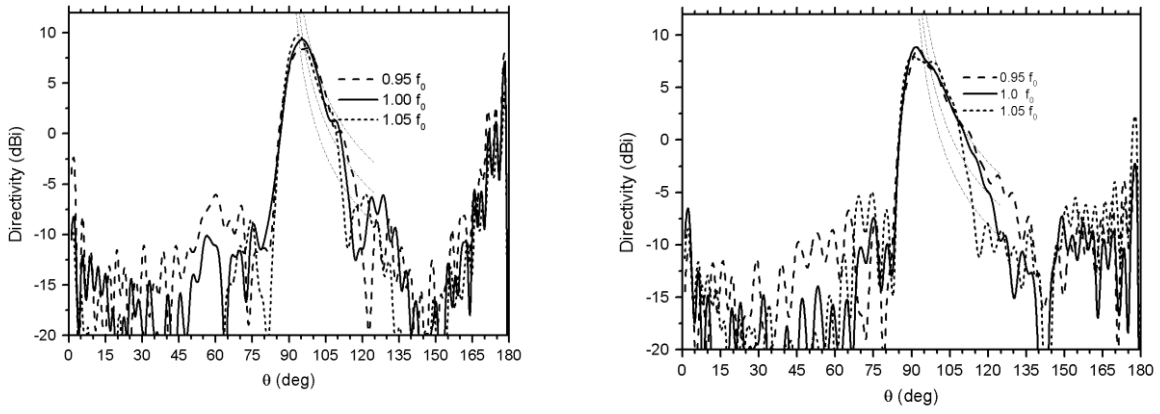

(a) (b)

Fig. 7. Radiation patterns of the shaped omnidirectional antennas depicted in (a) Fig. 6a and (b) Fig. 6b at the relative frequencies 0.95 f_o, f_o, and 1.05 f_o (MoM analyses).

Both ADC and ADE configurations were designed to offer a uniform coverage with a cosecant squared pattern given by (8) from $\theta = 93°$ to $\theta = 125°$. In other words, for the ADC with a main-reflector with a virtual caustic $\theta_2 = 93°$ and $\theta_1 = 125°$, while for the ADE with the real caustic $\theta_2 = 125°$ and $\theta_1 = 93°$. The cosecant squared pattern and its ±3 dB levels are shown in dotted lines in Fig. 7. Full-wave MoM analyses were conducted at the relative frequencies 0.95 f_o, f_o, and 1.05 f_o. The MoM radiation patterns of the shaped ADC and ADE are shown in Figs. 7a and 7b, respectively. From Fig. 7 one may observe the difficulty in sustaining the radiation pattern within the cosecant-squared specifications at $\theta \approx 120°$. This is basically due to the variation of the radiation pattern of the TEM coaxial feed horn with frequency. Table II lists the gain peak and location for each case.

Brazilian Microwave and Optoelectronics Society-SBMO received 25 Nov., 2008; revised 3 Feb., 2009; accepted 24 March, 2009
Brazilian Society of Electromagnetism-SBMag *ISSN 1516-7399*

Table II– Gain peak and location for each case .				
	ADE		ADC	
Frequency	G_{MAX}(dBi)	$\theta_{MAX}(^0)$	G_{MAX}(dBi)	$\theta_{MAX}(^0)$
$0.95f_0$	8.73	93	8.45	97
$1.0\ f_0$	8.88	92	9.34	95
$1.05f_0$	7.95	90	9.81	94

IV. CONCLUSIONS

This work discussed the bandwidth behavior of omnidirectional dual-reflector antennas derived from the ADC and ADE configurations. Initially, classical configurations where both sub- and main-reflector surfaces are generated by conic sections were considered. MoM analyses were conducted across a 10% bandwidth in order to investigate the broadband characteristics of the dual-reflector antennas. It was verified that the antenna gains were sustained across the 10% bandwidth with a maximum variation of 0.7 dB.

Shaped omnidirectional dual-reflector antennas were also investigated. Initially, a main-reflector synthesis procedure, based on GO principles, was presented. The main-reflector shaping procedure was then applied in two case studies where an ADC and an ADE were designed to provide a uniform omnidirectional coverage by means of a cosecant squared pattern in the elevation plane. Differently from the classical dual-reflector arrangements, the cosecant-squared specification was not sustained across the 10% bandwidth, basically due to the variation of the feed radiation pattern with frequency.

ACKNOWLEDGMENTS

This work was partially supported by CNPq, projects 470699/2006-0 and 310945/2006-2; FAPEMIG, 4859-6.01/07; CAPES, PROCAD 0377058; and FAPERJ, E-26/171083/03.

REFERENCES

[1] A. P. Norris and W. D. Waddoup, “A millimetric wave omnidirectional antenna with prescribed elevation shaping,” in Proc. ICAP—4th Int. Conf. Antennas and Propagation, 1985, pp. 141–145.

[2] M. Orefice and P. Pirinoli, “Dual reflector antenna with narrow broadside beam for omnidirectional coverage,” Electron. Lett., vol. 29, no. 25, pp. 2158–2159, Dec. 9, 1993.

[3] P. Besso, R. Bills, P. Brachat, and R. Vallauri, “A millimetric wave omnidirectional antenna with cosecant squared elevation pattern,” in Proc. ICAP—10th Int. Conf. Antennas Propagat., pp. 448-451, 1997.

[4] A. G. Pino, A. M. A. Acuña, and J. O. R. Lopez, “An omnidirectional dual-shaped reflector antenna,” Microw. Opt. Tech. Lett., vol. 27, no. 5, pp. 371–374, Dec. 5, 2000.

[5] J. R. Bergmann, F. J. V. Hasselmann, and M. G. C. Branco, ”A single-reflector design for omnidirectional coverage,” Microwave Opt. Tech. Lett., vol. 24, no. 6, pp. 426–429, March 20, 2000.

[6] J. R. Bergmann and F. J. S. Moreira, “An omni directional ADE reflector antenna,” Microwave Opt. Tech. Lett., vol. 40, no. 3, pp. 250–254, Feb. 5, 2004.

[7] F. J. S. Moreira and J. R. Bergmann, “Classical axis-displaced dual-reflector antennas for omnidirectional coverage,” IEEE Trans. Antennas Propagat., vol. 53, no. 9, pp. 2799–2808, Sep. 2005.

[8] F. J. S. Moreira and J. R. Bergmann, "Axis-Displaced Dual-Reflector Antennas for Omnidirectional Coverage with Arbitrary Main-Beam Direction in the Elevation Plane," IEEE Trans. Antennas Propagat., vol. 54, no. 10, pp. 2854–2861, Oct. 2006.

[9] B. S. Westcott, F.A. Stevens, F. Brickell, “GO synthesis of offset dual reflectors”, IEE Proc., Vol. 128, Pt. H, no.1, pp.11–18, Feb. 1981.

[10] S. Silver (ed.), *Microwave Antenna Theory and Design*, McGraw-Hill, NY, 1949.

Brazilian Microwave and Optoelectronics Society-SBMO received 25 Nov., 2008; revised 3 Feb., 2009; accepted 24 March, 2009
Brazilian Society of Electromagnetism-SBMag *ISSN 1516-7399*